Int. J. Adv. Eng. Pure Sci. 2023, 35(1): 100-115
DOI:10.7240/jeps.1224430

**RESEARCH ARTICLE** / ARAŞTIRMA MAKALESİ

# Numerical Optimization of Gas Cooler Geometry in Transcritical Refrigeration Cycles

*Transkritik Soğutma Çevrimlerinde Gaz Soğutucu Geometrisinin Sayısal Optimizasyonu*

**Ahmet Furkan URKUT[1], Efe Oğuzhan KARCI[2], Mehmed Rafet ÖZDEMİR[1]**

[1] *Department of Mechanical Engineering, Faculty of Engineering, Marmara University, 34854, İstanbul, Turkey*

[2] *Department of Mechanical Engineering, Boğaziçi University, 34342, İstanbul, Turkey*

**Abstract**
Traditional halocarbon – based refrigerants tend to considerably increase global warming and ozone depletion factors. Therefore, $CO_2$ is fast becoming a key instrument as a natural refrigerant which was widely applied and attracted the consideration of the research community. The gas cooler is a critical component in the $CO_2$ transcritical refrigeration system and plays a major role in the performance due to the determination of operating pressure consequently power consumption. In this research, the performance characteristics of a $CO_2$ gas cooler having wavy fin geometry, which is currently employed in industries including air conditioning, automotive and aviation, was determined experimentally in a calorimetric test room. The experimental results was used as benchmark data to validate the three – dimensional numerical model. Laminar model and realizable k - ε turbulent model were employed for analyses. Moreover, the second order upwind scheme was considered to discretize momentum and energy equations. Accordingly, a multi-objective optimization process has been performed employing Response Surface Method (RSM) to determine the optimum wavy fin geometry in $CO_2$ transcritical refrigeration system. Four geometrical parameters namely longitudinal pitch, half transverse pitch, tube outer diameter, and fin pitch of the gas cooler were optimized. According to results, the new optimized $CO_2$ gas cooler exhibited lesser pressure drop and higher heat transfer capacity in comparison with the tested gas cooler geometry used in the industry. It was appeared that the overall heat transfer coefficient enhancement is between 5.4 – 12.2 % while pressure drop decreases about 175.08 – 188.58 % for three different inlet velocities.
**Keywords:** natural refrigerants, heat transfer coefficient, gas cooler, optimization, wavy fin

**Öz**
Geleneksel halokarbon bazlı soğutucu akışkanlar, küresel ısınmayı ve ozon tabakasını inceltme faktörlerini önemli ölçüde artırma eğilimindedir. Bu nedenle, araştırma topluluğunun dikkatini çeken ve hızla yaygın olarak uygulanan doğal bir soğutucu olarak $CO_2$ önemli bir araç haline gelmektedir. Gaz soğutucu, $CO_2$ transkritik soğutma sisteminde önemli bir bileşendir ve çalışma basıncının ve dolayısıyla güç tüketiminin belirlenmesi nedeniyle performansta önemli bir rol oynar. Bu araştırmada, günümüzde iklimlendirme, otomotiv ve havacılık gibi sektörlerde kullanılan dalgalı kanatçık geometrisine sahip bir $CO_2$ gaz soğutucunun performans özellikleri kalorimetrik bir test odasında deneysel olarak belirlenmiştir. Deneysel sonuçlar, üç boyutlu sayısal modeli doğrulamak için ölçüt olarak kullanılmıştır. Analizler için laminer model ve realizable k - ε türbülanslı model kullanılmıştır. Ayrıca momentum ve enerji denklemlerini ayrıklaştırmak için second order upwind şeması kullanılmıştır. Buna göre, $CO_2$ transkritik soğutma sisteminde optimum dalgalı kanatçık geometrisini belirlemek için Yanıt Yüzey Yöntemi (RSM) kullanılarak çok amaçlı bir optimizasyon işlemi gerçekleştirilmiştir. Gaz soğutucunun boyuna hatvesi, yarım enine hatvesi, boru dış çapı ve kanatçık hatvesi olmak üzere dört geometrik parametre optimize edilmiştir. Sonuçlara göre, yeni optimize edilmiş $CO_2$ gaz soğutucusunun, endüstride kullanılan test edilmiş gaz soğutucu geometrisine kıyasla daha az basınç düşüşü ve daha yüksek ısı transfer kapasitesi sergilediği görülmüştür. Üç farklı giriş hızı için ortalama ısı transfer katsayısı iyileşmesinin %5,4 – 12,2 arasında olduğu, basınç düşüşünün ise % 175,08 – 188,58 oranında azaldığı görülmüştür.
**Anahtar Kelimeler:** doğal soğutucular, ısı transferi katsayısı, gaz soğutucu, optimizasyon, dalgalı kanatçık

**Corresponding Author:** Mehmed Rafet Özdemir, Tel: 02167773739, e-posta: mehmet.ozdemir@marmara.edu.tr
**Submitted:**26.12.2022, **Revised:** 28.02.2023, **Accepted:** 17.03.2023

# I. INTRODUCTION

Development of the industry has considerably increased environmental pollution and global warming issues over the past decades. With the Montreal and Kyoto protocols, industries and developing countries have adopted a number of legal regulations. Until these protocols, the selection of refrigerants used in the refrigeration systems was based on economic and efficiency factors while concerns about environment were not seriously considered. On the other hand, the ozone depletion and global warming factors of halocarbon – based refrigerants are very high. For instance, global warming potential of Halocarbon based refrigerant R23 is 11700 times higher than natural refrigerant Carbon dioxide ($CO_2$) [1]. When awareness over the environmental damage of these halocarbon-based refrigerants like Chlorofluorocarbon and Hydrochlorofluorocarbon (CFCs, HCFCs) arose in the 1990s, natural refrigerants such as $CO_2$ were reintroduced to the industry. However, most of these natural refrigerants cannot satisfy the performance and safeness criteria [2]. For instance, ammonia is flammable and toxic, thereby, not qualified for certain operations [3]. Another natural refrigerant example can be regarded as water. It is easily available and non-toxic but it has low operating pressure and density, henceforth water is not a good nominee for vapour compression refrigeration systems [4]. Also, water may not be considered cost-effective because of its low heating coefficient of performance (COP) [5]. $CO_2$ is one of the non – flammable and non – toxic natural refrigerant [3]. Also, $CO_2$ can be discharged to the atmosphere and it doesn't need to be retrieved. Furthermore, $CO_2$ has no ozone depletion potential and therefore the governmental regulations don't be applied to it. Besides, $CO_2$ has higher density, thermal conductivity, latent heat and specific heat, and smaller viscosity as against Hydrofluorocarbons (HFCs) which are widely used today. Moreover, thanks to its negligible global warming potential and environmentally friendly features, $CO_2$ is not tend to be phased out unlike HFCs [6]. The use of $CO_2$ in refrigeration systems is cost – effective since exists aplenty in the atmosphere [2]. Moreover, $CO_2$ can be considered as a safe refrigerant according to the safety standards of ISO 5149 and ASHRAE 15 and 34 [3]. In consequence, the leakage into the atmosphere of $CO_2$ is regarded as very minimum.

The $CO_2$ refrigerated cooling systems have been used in various applications such as ice cream freezers, cold beverage vending machines, supermarket refrigeartion systems, heat pumping units and food retailing [7,6]. For a more sustainable life, this kind of environmentally friendly cooling systems need to be developed and widely employed. In refrigeration systems, $CO_2$ gas in the transcritical zone forces the system to operate in single phase. Since two-phase condensation does not occur, the system has gas cooler rather than the condenser. Therefore the gas cooler is the responsible equipment for the heat transfer to the ambient. The COP of the system is augmented with the presence of the additional internal heat exchanger in the cycle. The temperature gradient in the gas cooler directly affects the COP value [8]. In this context, the gas cooler can be considered very important equipment in the $CO_2$ transcritical cooling cycle. Therefore, the relevant literature has been examined below to present the knowledge about the impacts of gas cooler fin geometry and fin arragement on heat transfer and pressure drop behaviours.

Jang and Chen [9] numerically examined the heat transfer and pressure drop behaviours of a wavy finned – tube heat exchanger for various geometrical parameters including wavy heights, wavy angles and tube row numbers for Reynolds number (Re) varying from 400 to 1200. The findings revealed that wavy fin arrangement has higher Colburn factor than plain fin arrangement within a range of 63%-71% and also wavy fin arrangement has 75% to 102% higher friction factor values. When wavy height was kept constant, the pressure and average Nusselt number (Nu) raise with growing wavy angle. However, the wavy height has an adverse impact on the pressure drop and average Nu at the constant equal wavy angle. They also observed that row effect is not significant for wavy fin compared to the plain fin. In another research, Kim and Bullard [10] carried out sets of experiments in a flat tube and multi – louvered fin heat exchangers to investigate the airside pressure drop and heat transfer attributes. Experiments were performed for different pitches, flow rates and louver angles for Reynolds number ranging between 100 and 600. The friction coefficient and colburn j-factor were defined in terms of Re number function in heat exchangers of different geometric configurations. The correlation created for the friction factor showed that the most important parameter in the pressure loss is the flow depth. Besides, results showed that the heat transfer coefficient (HTC) augments substantially with air velocity and decreases with flow depth. They observed that pressure drop increases with raise in louver angle and flow depth and decreases with rise in fin pitch. Mon and Gross [11] numerically studied the effect of fin spacing in annular finned four-row tubes having in-line and staggered configurations. Analyses were executed for Reynolds number ranging between 8600 and 43000. It was reported that the pressure loss diminished with the raise in the ratio of fin spacing to height for both tube arrangements. HTC enhanced with the ratio of fin spacing to a height up to the certain value (0.32),

afterwards it was nearly constant for staggered tube arrangement. On the other hand, the HTC showed an increasing trend in the entire range for the in-line configuration. Tao et al. [12] examined the fin efficiency, heat transfer characteristics and temperature pattern on the surface of the fin in tube and wavy-fin heat exchangers using a three-dimensional numerical model for various wavy angles changing from 0° to 20°. The three-dimensional numerical analyses were carried out by employing body-fitted coordinates (BFC) methodology which considers the fin efficiency influence in the model. Findings showed that plain plate has lower fin efficiency than the wavy plate at the inlet region. They also reported that as the Reynolds number increases the impact of wavy angle on the fin efficiency and local Nusselt number become more significant. Lu et al. [13] analysed the effects of tube pitch, tube diameter, fin pitch and fin thickness on the air-side characteristics of staggered finned tube heat exchangers numerically. The results explained in terms of heat transfer rate over pressure drop. It was seen that COP of the heat exchanger declines with increasing tube diameter and fin thickness whereas it increases with increasing tube pitch. Dong et al. [14] performed experiments to analyse the thermal-hydraulic characteristics of the airside in the flat tube and wavy fin aluminium heat exchanger for different working conditions and wavy fin geometry parameters. They conducted the multiple regression method to develop pressure loss and heat transfer correlations in the heat exchanger. Furthermore, the parametric study by applying the Taguchi method was managed to examine the thermal-hydraulic performances of the wavy fins. The study indicated that the amplitude and the length of the wavy fin are very significant parameters affecting the total thermal-hydraulic performance of the heat exchanger. They reported that decrease in fin pitch and fin length would enhance the heat transfer performance. Santosa et al. [15] numerically and experimentally studied the local HTC of refrigerant and air sides of the $CO_2$ gas cooler with the finned tube. Studies were performed on two gas cooler designs, each with or without slit on the fins. It was observed that adding a slit between rows increases the heat transfer by preventing heat transmission among the tubes. They reported that adding slit enhances the heat rejection rate between 6% and 8%. As a consequence of this study, it was seen that computational fluid dynamics (CFD) modelling is an accurate and effective simulation tool for air and refrigerant side calculations. In another study, Zhang et al. [16] developed a three-dimensional CFD model of a flat finned tube gas cooler. The airside model was designed with 2 fins and 54 tubes, while the refrigerant-side model was designed with 10 fins and 54 tubes. They observed that as inlet velocity increases the temperature of the refrigerant decreases. Javaherdeh et al. [17] numerically and experimentally analysed the effects of louver length, fin height and thickness of fin-tube contact on the pressure loss and heat transfer performance in a louvered fin and tube heat exchanger. Results revealed the performance of heat exchanger enhanced when the thickness of the fin-tube contact was increased until the contact thickness equals to fin thickness. However, a further increment in the thickness of the fin-tube contact did not affect the heat exchanger performance. Moreover, when the louver length was increased at a fixed fin height the performance of heat exchanger enhanced. In the study carried out by Zhang et al. [18], a three-dimensional CFD model was utilized to examine the airside pressure drop and HTC, heating capacity and inlet temperature in $CO_2$ finned tube gas cooler for different inlet velocity ranges of airflow. They observed that, the best performance has been achieved with uniform airflow pattern by having the largest heat capacity, the smallest pressure drop, the lowest approach temperature and the highest COP.

The aforementioned literature review shows that there are many geometric factors such as tube diameter, fin height, fin pitch, wavy angle and fin thickness affect the performance of gas cooler in $CO_2$ transcritical refrigeration systems. However, the number of systematic studies considering all these parameters is very scarce in the literature. Thus, further researches are needed to elaborate on the effect of geometrical parameters on the performance of gas coolers in $CO_2$ transcritical refrigeration systems. This particular study presents a numerical CFD research on optimization of the gas cooler geometry considering longitudinal pitch ($P_L$), half transverse pitch ($P_T/2$), fin collar outside diameter ($D_c$) of tube and fin pitch ($F_P$) and investigates effects of these parameters on heat transfer capacity of the gas cooler in $CO_2$ transcritical refrigeration systems. The numerical model has been analysed for airside of the gas cooler and validated with the experimental tests using the gas cooler geometry having wavy fin with circular tube. Thereafter, an optimization study was conducted along with the gas cooler geometry using response surface method (RSM). The heat transfer and pressure loss data of the optimized gas cooler geometry results were compared with experimental findings.

# II. MATERIALS AND METHODS

## 2.1. Test Rig and Experimental Investigation

The test rig was employed to validate the numerical model in the current study. The gas cooler was tested in environment-balanced type calorimetric test room according to the EN 327 [19] and EN 328 [20] standards. The gas cooler was made of aluminium fins with wavy fin type. Table 1 presents the properties of the tested gas cooler. The calorimetric test room was located in the conditioning chamber to prevent any heat exchange from the environment. The test room consists of a $CO_2$ refrigerant line, data acquisition system and air control unit. The temperature and humidity was adjusted with air control unit in the test room.

Figure 1 depicts the details of the $CO_2$ refrigerant line schematically. The $CO_2$ refrigerant line consists of a separated tank, evaporator, two parallel transcritic compressors with a controllable capacity (Bitzer 4HTC-15K-40P), water line, subcooler, precooler, data acquisition System (Agilent 34970A), coriolis flow meter (Krohne Optimass 1400), refrigerant control systems (Danfoss AK-PC 720, EKD 326) and ICMT high pressure valve which is a motorized valve driven by an actuator. The tank is used at medium pressure as a separator to separate the gas and liquid phases of the $CO_2$ refrigerant in the system. The liquid phase is collected in the lower part of the tank and it is reduced to the evaporation pressure in the expansion valve and enters the evaporator at quality of 0.25-0.3. The liquid $CO_2$ evaporates according to the superheating value set by the electronic control system by withdrawing the heat of the auxiliary line water at constant pressure. The compressor suction is fed with the $CO_2$, which occurs at the gas phase after high-pressure throttling, and the $CO_2$ gas supplied from the evaporator. Thereafter, the $CO_2$ is compressed in the compressor (8000-9500 kPa) and delivered to the prototype gas cooler. The temperature of the $CO_2$ gas is reduced by discharging heat to the environment at constant air inlet temperature and constant fluid pressure.

The 18 kW heater and 36 kW chiller in the air conditioning unit were used to adjust the humidity and temperature of the inlet air using PID control system with the incoming data from the sensors. It was ensured that the system reached a steady-state before collecting the data. In steady-state condition, the test performance of the gas cooler was measured until it reaches ± 4% of the total cooling and heating loads given to the test room. The temperature and pressure data of the $CO_2$ were measured at the upstream and downstream of the gas cooler. The Reynolds number (Re) was determined using the inlet velocity of air where the characteristic length is the hydraulic diameter ($D_H$) of the tube. The $D_H$ and Re are defined in equation (1) and equation (2) respectively.

**Table 1.** Gas cooler properties

| | |
|---|---|
| Transverse pitch ($P_T$) | 25.4 mm |
| Longitudinal pitch ($P_L$) | 22 mm |
| Fin pitch ($F_P$) | 2.5 mm |
| Fin type/fin thickness (t) | Wavy/0.1 mm |
| Fin material | Aluminium |
| Tube material | Copper |
| Tube wall thickness | 0.55 mm |
| Inner diameter of the tube ($D_{in}$) | 7.94 mm |
| Fin collar outside diameter ($D_c$) | 9.04 mm |
| Row number | 3 |
| Total pipe number | 60 |
| Total fin number | 480 |
| Circuit number | 6 |
| Length | 1200 mm |
| Air volumetric flow ($\dot{m}_{air}$) | 1.66 kg $s^{-1}$ |

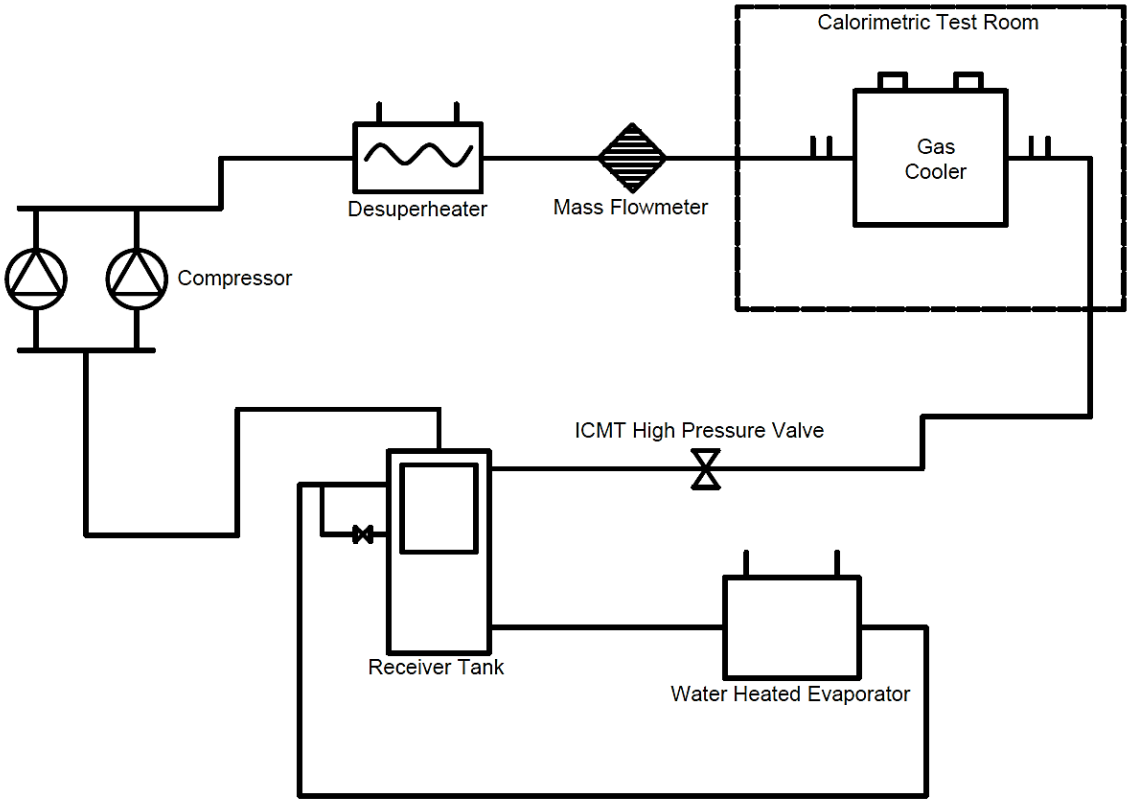


**Figure 1.** Schematic of the $CO_2$ refrigerant line

$$D_H = \frac{2F_P P_T}{F_P + P_T} \tag{1}$$

$$\mathrm{Re} = \frac{\rho u D_H}{\mu} \tag{2}$$

$$\dot{Q} = \dot{m}_{air} \times \left(e_i - e_o\right) \tag{3}$$

$$h_{air} = \frac{\dot{Q}}{A_{tot}\left(T_w - T_b\right)} \tag{4}$$

Where $\rho$ signifies the fluid density, $u$ denotes velocity and $\mu$ represents the dynamic viscosity. The heat transfer rate, $\dot{Q}$ and consequently the airside HTC, $h_{\mathrm{air}}$ in each part is computed using following equations.

In Equation (3), $e_i$ and $e_o$ are inlet and outlet enthalpy of the air for the relevant temperature and pressure

respectively and $\dot{m}_{air}$ is the mass flow rate of the air. In equation (4), $A_{tot}$ denotes the total heat transfer surface area including collars and fins whereas $T_w$ designates average wall temperature value which is the average of collar temperature and fin temperature. Also, $T_b$ is the bulk air temperature which can be described as average air upstream and downstream temperature.

The propagated uncertainty analysis was also conducted during the experiments according to the method explainedin ref. [21]. The uncertainty values were ±5.1 – 10.9 % for the total cooling capacity and ±3.2 –9.1 % for pressure drop. The inlet velocity of the fan was considered constant during the experiments (2.55 m $s^{-1}$). The experiment was conducted several times to check the repeatability of the experiment and it was found that the experimental results are very well agree with each other for all cases.

Mean absolute error (MAE) was used to present the prediction capability of the numerical model for the experimental data. The MAE in percentage can be defined with the following equation. In the below equation, $f_i$ denotes the numerical result, $y_i$ stands for the experimental result and $n$ is the number of data.

$$MAE = \frac{1}{n}\sum_{i=1}^{n}\frac{|f_i - y_i|}{y_i} \times 100\% \tag{5}$$

**2.2. Numerical Analysis**

The tested gas cooler whose properties given in Table 1 was adopted for the numerical model. Three-dimensional geometry of the tested gas cooler was sketched in computer aided design (CAD) environment. Then the CFD model of the geometry was generated by the aid of the ANSYS® Fluent commercial software package. The software is originated by finite volume principle. The laminar models with simple and coupled algorithms and realizable k-Ɛ turbulent flow using the standard wall model were applied to elaborate the heat transfer and fluid flow features at various inlet velocities. The flow was considered to be steady and incompressible during the analysis. The second-order upwind model was employed to discretize the energy and momentum equations. Therefore, the pressure-based continuity and momentum equations were solved accurately by this coupled algorithm. It should be noted that this pressure-based coupled algorithm provides some benefits compared to the pressure-based segregated algorithm in terms of having more powerful and accurate solutions for steady-state flows [22]. The CFD model solves the conversation of mass, energy and momentum equations to characterize heat transfer and fluid flow in the gas cooler. Governing equations used in the simulations are shown below.

Conservation of mass (continuity):

$$\frac{\partial}{\partial x_i}\left(\rho u_i\right) = 0 \tag{6}$$

Conservation of momentum:

$$\frac{\partial}{\partial x_j}\left(\rho u_i u_j\right) = -\frac{\partial P}{\partial u_i} + \frac{\partial \tau_{ij}}{\partial x_j} \tag{7}$$

$$\tau_{ij} = \mu\left(\frac{\partial u_i}{\partial x_j} + \frac{\partial u_j}{\partial x_i}\right) - \frac{2}{3}\mu\frac{\partial u_k}{\partial x_k}\delta_{ij} \tag{8}$$

Conservation of energy:

$$\frac{\partial}{\partial x_i}\left(u_i\left(\rho E + P\right)\right) = \frac{\partial}{\partial x_i}\left(\lambda\frac{\partial T}{\partial x_i}\right) \tag{9}$$

Where $\tau_{ij}$ signifies the stress tensor, $\lambda$ denotes the thermal conductivity, $E$ indicates the total energy, $P$ represents the pressure and $T$ denotes the temperature; $i$, $j$ and $k$ signify subindexes of the cartesian coordinate system.

The below assumptions were applied during analysis since the complexness and computational CPU cost become very large to model the entire gas cooler.

a- The each circuit were assumed to run as individual gas cooler interrelated with each other in parallel as shown in Figure 2. Because the experiments indicate that the temperature and performance data of each circuit exhibited similar characteristics.

b- The temperature of tubes was considered constant temperature of 318.15 K. This temperature value is the average temperature during experiments and reasonable since it is above the critical point of $CO_2$. This assumption also enables us to divide each circuit into several segments along the pipe length to simplify CFD model reasonably.

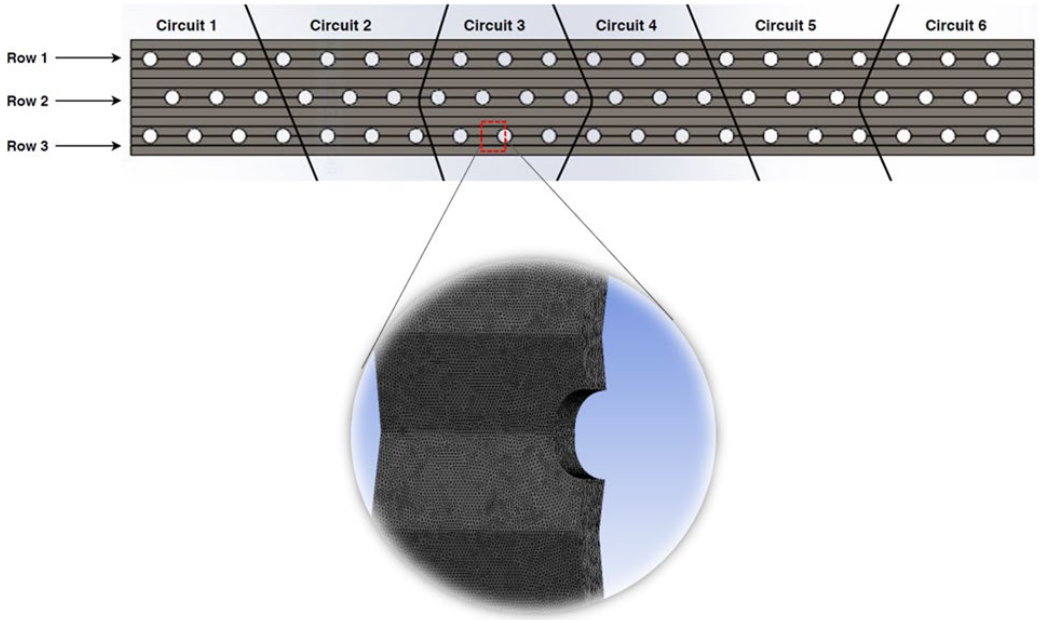


**Figure 2.** Top view of the CAD geometry of the gas cooler with rows and circuits and the grid structure of the model

Accordinlgy, the CFD domain can be regarded as in Figure 3. Moreover the domain was extended to cover input and output regions of the model to have uniform 1-D velocity profile at the entrance and to prevent backflow at the outlet of the model. This method is also very common in literature to avert from the effect of reversed flow, as encountered by the solver and widely stated in literature, see for example refs. [23-25]. In this study, the extension length was set equal to longitudinal pitch at the inlet section and two times longitudinal pitch length at the outlet section. These extension lengths were considered while calculating cooling capacity which are presented in results and discussion section. Moreover, the fins and tubes were modelled as thin walls in the CFD model. The oulet pressure of the model was assumed as gauge pressure during the solution. In the computational solution, the fins were treated as solid and no-slip boundary condition with the periodic condition was implemented to the lower and upper walls of fins. The inlet air temperature between two fins was set to a constant temperature of 302.15 K considering the experimental conditions of tested gas cooler. Moreover, the symmetry boundary condition was assumed at the lateral surfaces of the model. The convergence criterion has been defined as $10^{-9}$ for momentum and energy equations whereas it was set to $10^{-6}$ for continuity equation. Flow chart of the numerical model was illustrated in Figure 4.

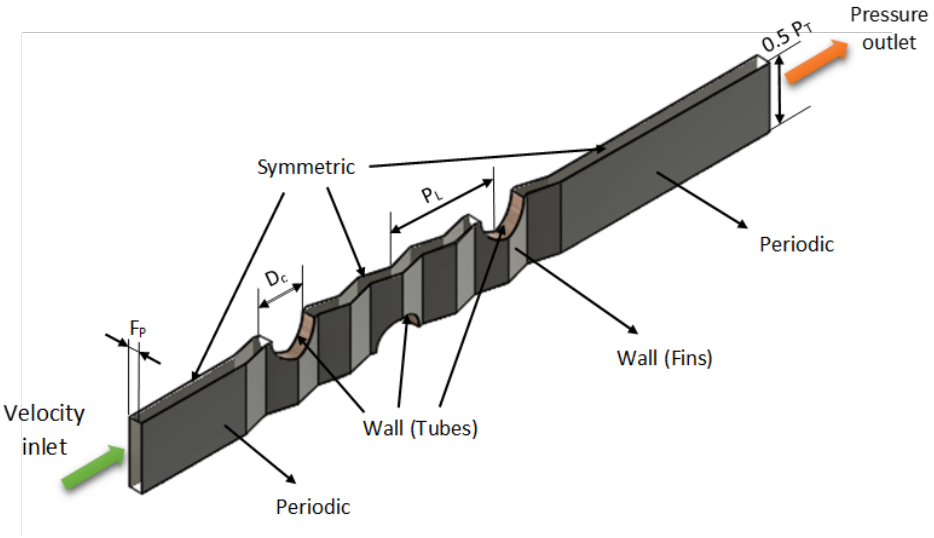


**Figure 3.** CFD domain of wavy fin and circular tubes

The mesh generation process is a crucial stage in CFD works since meshing could influence the reliableness, convergence and consistency of the results. The tetrahedral grid scheme was used to obstruct any potential ill-shaped cell in the CFD domain as can be seen in Figure 2. The grid scheme consists of 46957 nodes and 228724 tetrahedral elements. Moreover, the fully automatic meshing procedure was used with small element size (0.5 mm) for the faster and more accurate solution. The CFD domain was divided into several subdomains considering mesh structure and number to save computational and convergence time in the solution. The mesh quality of the computational domain is dependent on the skewness and orthogonal qualities of meshes. It was found that the average orthogonal quality of the meshes is 0.77. On the other hand, the average skewness and maximum skewness values of the meshes were 0.2 and 0.6 respectively. These values are in agreement with the results of [26-28], which stated that the average skewness value is in the range of 0.1 and 0.5 whereas the maximum skewness value varies from 0.5 to 0.75 for good quality meshes. Accordingly, different size and number of meshes were employed to perform mesh independency study and results of pressure drop and HTC are demonstrated using five different grids in Table 2 below. Table 2 presents that the difference of the overall HTC which is denoted as $h_{av}$ and pressure drop ($\Delta P$) values for the five meshes is insignificant. Accordingly, the medium mesh is adopted for the analysis.

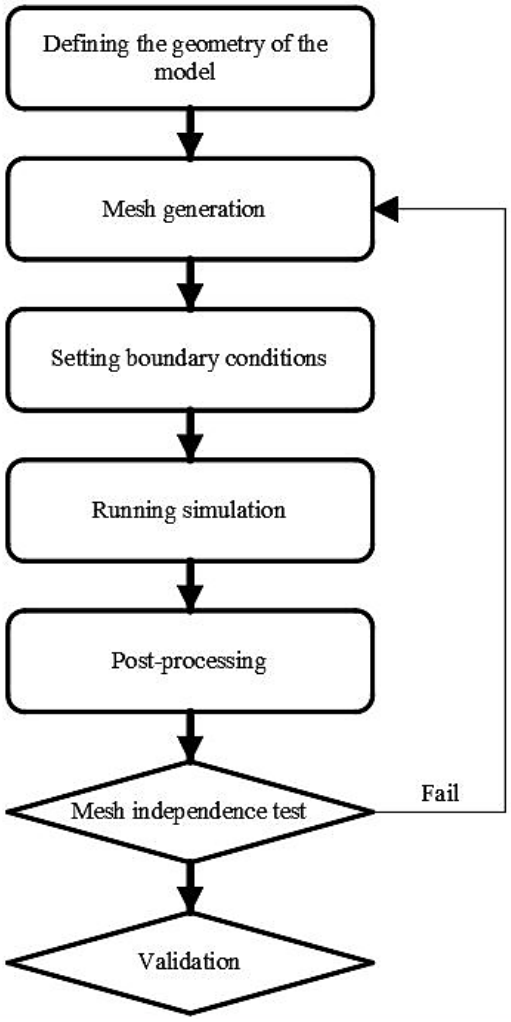


**Figure 4.** Flow chart of the numerical model

**Table 2.** Mesh independency results

| Grid number [-] | $h_{av}$ [Wm$^{-2}$K$^{-1}$] | ΔP [Pa] |
|---|---|---|
| Coarse grid | 12.6454 | 5.37741 |
| Medium grid | 12.6542 | 5.38201 |
| Fine grid | 12.6338 | 5.3824 |
| Finer grid | 12.6452 | 5.39427 |
| Finest grid | 12.6505 | 5.38792 |

### 2.3. Optimization Process

In this study, a multi-objective optimization process was integrated with the response surface method (RSM), design of experiments (DOE), multi-objective genetic algorithm (MOGA) and CFD model to design optimum gas cooler geometry in $CO_2$ transcritical refrigeration systems. This algorithm was concucted with regards to the different geometrical parameters of gas cooler in terms of the Non-dominated sorting genetic algorithm II (NSGA-II) method [29]. This model generates 4000 samples initially, 800 samples per iteration and accordingly presents 3 candidate design points in maximum of 20 iterations. It was found that the solution converged after 12064 evaluations.

The RSM and genetic algorithm (GA) were used to carry out the optimization study. The RSM was first developed by Box and Daper [30] for designing experiments and optimizing the effect of mix parameters [31, 32]. Accordingly, the objective function of RSM algorithm can be formulated in Equation (10).

$$Y = \beta_0 + \sum_{i=1}^{n} \beta_i X_i + \sum_{i=1}^{n} \sum_{j=1}^{n} \beta_{ij} X_i X_j + \ldots \qquad (10)$$

Where $\beta_0$, $\beta_i$ and $\beta_{ij}$ are tuning parameters, Y is the response variable and $n$ is the number of parameters.

In the current work, because of the non-uniformity of the HTC at the fin surface, it was very complicated to measure the local HTC on the fins, therefore the local heat flux and local fin temperature are need to be evaluated [33]. The objective functions were defined as maximum HTC through the gas cooler considering surface of the fins and surface of the tubes together, minimum pressure drop and maximum heat flux in the gas cooler which are developed a correlation function with four design variables namely longitudinal pitch, fin pitch, half of the transverse pitch and tube diameter of the gas cooler. The objective functions namely $f_1$, $f_2$ and $f_3$ and constraints are defined as follows:

$$Maximize\ h_{local} = f_1(P_T/2, P_L, F_P, D_c) \qquad (11)$$

$$Maximize\ \Phi = f_2(P_T/2, P_L, F_P, D_c) \qquad (12)$$

$$Minimize\ \Delta P = f_3(P_T/2, P_L, F_P, D_c) \qquad (13)$$

$$Constraints: 10\ mm \le P_T/2 \le 15\ mm;\ \ 15\ mm \le P_L \le 25\ mm;\ \ 2\ mm \le F_P \le 3\ mm;\ \ 5\ mm \le D_c \le 12\ mm. \qquad (14)$$

Where $h_{local}$ is the local HTC and $\Phi$ is the local heat flux. The lower and upper limits of the constraints were defined for design variables considering the design limitation of the gas coolers in the industry. The design constraints can be comprehended clearly by analysing Figure 3.

After defining the objective functions and design variables, the numerical optimization problem was solved using RSM and MOGA methods to reveal optimum geometries and arrangement. The Central Composite Design (CCD) which is an algorithm of DOE method is used to obtain sample data points. Consequently, a best combination of design variables in the range described in equation (14) leading to minimum pressure drop and maximum heat transfer was determined. The best combination was chosen as the optimum geometry and

arrangement. The optimization procedure can be summarized as follows:

1- Determination of objective functions and design variables.
2- Application of DOE method to obtain optimal arrangement of design points.
3- Determination of the response surface from DOE results for each output parameter.
4- Solution of the objective function values with CFD.
5- Obtaining the objective functions according to the input parameters based on multi-objective genetic algorithm method.
6- Obtaining the optimum geometry among candidate points.

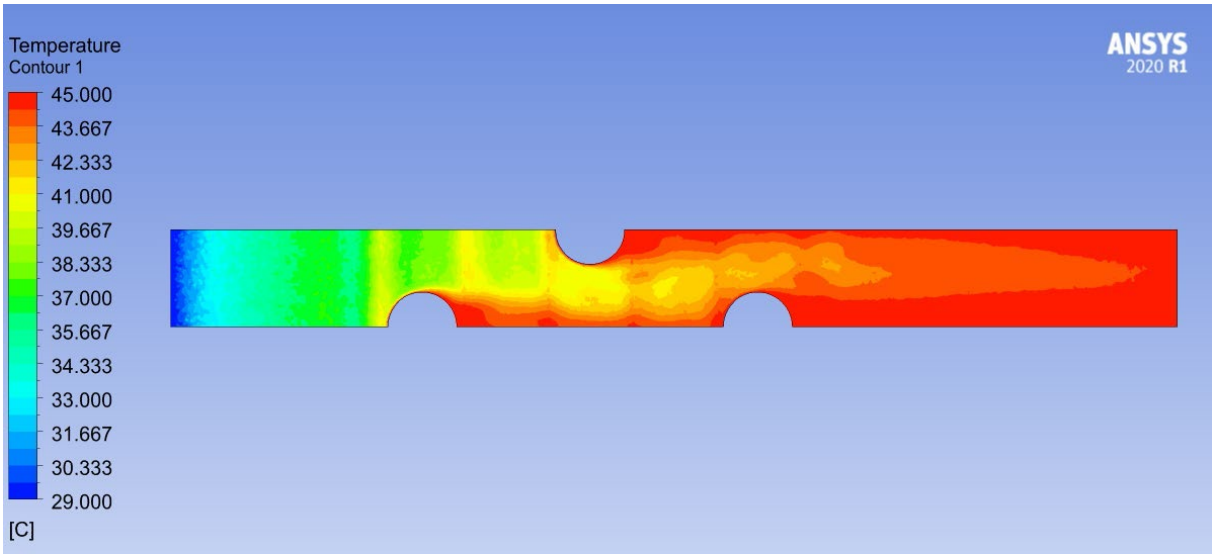


**Figure 5.** Temperature contour of the numerical model of the tested gas cooler at 1 m $s^{-1}$

## III. RESULT AND DISCUSSION

The numerical model of the gas cooler was validated using current experimental data. As can be seen from Table 3, the cooling capacity of the gas cooler ($\dot{Q}_{gc}$) predicted well by the numerical model. Although the MAE is 9.97 % for the total heat capacity between experimental test and numerical model, all data is in experimental uncertainty range which were ±5.1 – 10.9 %. Therefore, it can be stated that the numerical model can be used to analyse the gas cooler geometry in the current $CO_2$ transcritical refrigeration system.

**Table 3.** Comparison of the numerical model with experiment at u = 2.55 m $s^{-1}$

| | $\dot{Q}_{gc}$ [kW] |
|---|---|
| Experiment | 16.446 |
| Numerical model | 14.765 |
| MAE | 9.97 % |

Accordingly, the optimization process was performed for the validated numerical model. As stated in the materials and method section, the geometric parameters for the optimization process were chosen as longitudinal pitch, fin pitch, half of the transverse pitch and tube diameter of the gas cooler. The reason for choosing these geometrical parameters can be understood by analysing temperature and pressure contours of the gas cooler which was obtained via numerical model, please see Figure 5. As can be figured out from Figure 5, the temperature contours are not uniform and affected by the number of tubes, the arrangement of tubes, the spacing between tubes and diameter of tubes. These trends confirm that the abovementioned design parameters are effective in the total heat capacity and pressure drop performance of the gas cooler in the current system. Also, prior studies that have stated the importance of number of tubes consequently longitudinal pitch, fin pitch, half of the transverse pitch and tube diameter of the gas cooler greatly affect the thermal and pressure drop behaviour of the gas cooler [34-37].

The impact of each design parameter on the objective functions has been analysed separately in Figure 6 (a-h). It is worth to mention that the other design parameters were held constant to observe the

single effect through Figure 6 (a-h). As can be noticed from Figure 6 (a), the pressure loss through the gas cooler increases exponentially (~%85) and the HTC on the fin surface, $h_{local,f}$ increases slightly (~% 6) with the tube diameter was increased from 5 mm to 12 mm. On the contrary, the HTC on the tube surface, $h_{local,t}$ decreases (~% 15) with the raise in the tube diameter, see Fig. 6 (b). These findings also accord with our earlier studies, which indicated that the pressure loss rises with the tube diameter [13, 37 – 39] for plate fin and tube heat exchangers. The reason of this trend can be attributed to the enhancement of the wake region behind the tube wall as the tube diameter increases. Consequently, the air – side pressure drop increases. Furthermore, the heat transfer area and fin efficiency rises as the tube diameter enlarges which leads to higher HTC values at the fin surface. On the other hand, the HTC at the tube surface has a decreasing trend when the tube diameter was increased. This trend is expected since the growth in the tube diameter would result in shorter boundary layer development from the inlet of the fin and that results in poor heat transfer performance.

The effect of fin pitch on the pressure drop, fin surface heat transfer and tube surface heat transfer characteristics can be represented in Figure 6 (c-d). As the fin pitch was increased, the surface HTC on the tube and fin also augmented whereas the pressure loss through the fin decreased. Previous studies have also revealed that the fin pitch has significant impact on the HTC on the tube and fin similar to this study [11, 37, 40]. Because, the fin pitch distance largely affects the boundary layer development in the system. If the fin pitch becomes large, the boundary layers between the fins would diverge from each other consequently the heat transfer process becomes more effective. For smaller fin pitch values, the fluid can be utilized as trapped in the wake region so that this region cannot contribute to heat transfer process due to its small area. However, the region becomes larger as the fin pitch was enlarged and the circulation of the fluid becomes faster that results in better heat transfer rate. Romero-Méndez et al. [37] and Mon and Gross [11] stated that the heat transfer rate is higher at the larger fin pitch values due to the emergence of horseshoe type vortex. The decreasing pressure drop trend with the raise in the fin pitch distance can be attributed to the weak interactions of boundary layers between the fins as expected. Romero-Méndez et al. [37] showed that the flow around the rear of the tube was separated with the formation of a wake region with a recirculation zone.

Figure 6 (e-h) demonstrate the effect of tube spacing, namely longitudinal and transverse pitches, on the pressure drop and HTC on the fin surface and tube surface. The pressure drop through the system slightly decreased or wasn't influenced by the increase in longitudinal pitch whereas it decreased almost linearly when the transverse pitch was increased, see Figure 6 (e, g). As the transverse pitch was decreased, the fin tip clearance becomes smaller which results in higher velocity consequently larger pressure drop. The tube arrangement has a strong effect on the airflow characteristic and consequently affects heat transfer through the tube banks. The HTC decreased as the transverse pitch rises for both tube and fin surfaces. The reason behind this trend can be explained by the fact that the effect of tubes exerted on each other is reduced by enlarging transverse pitch. In this case, the tube banks would behave like individual finned tubes that results in lower HTC compared with the closer transverse pitch case. These findings agree with those of earlier studies [11, 13, 41, 42].

The abovementioned discussions reveal that the performance of the gas cooler can be affected by several geometric parameters. Consequently, the mixed effect of these parameters should be studied to find the optimum geometry of the gas cooler with the highest thermal-hydraulic performance. As mentioned before, the RSM and MOGA techniques were used in optimization process to uncover the mixed effect of design parameters on the objective functions. Consequently, the optimum gas cooler geometry dimensions can be presented in Table 4.

**Table 4.** Optimum Gas cooler dimensions

| | |
|---|---|
| Transverse pitch($P_T$)/ Longitudinal pitch ($P_L$) | 1.26 |
| Fin type/fin thickness (t) | Wavy/0.1 mm |
| Fin pitch ($F_P$) | 3 mm |
| Fin collar outside diameter ($D_c$) | 5 mm |
| Tube wall thickness | 0.55 mm |

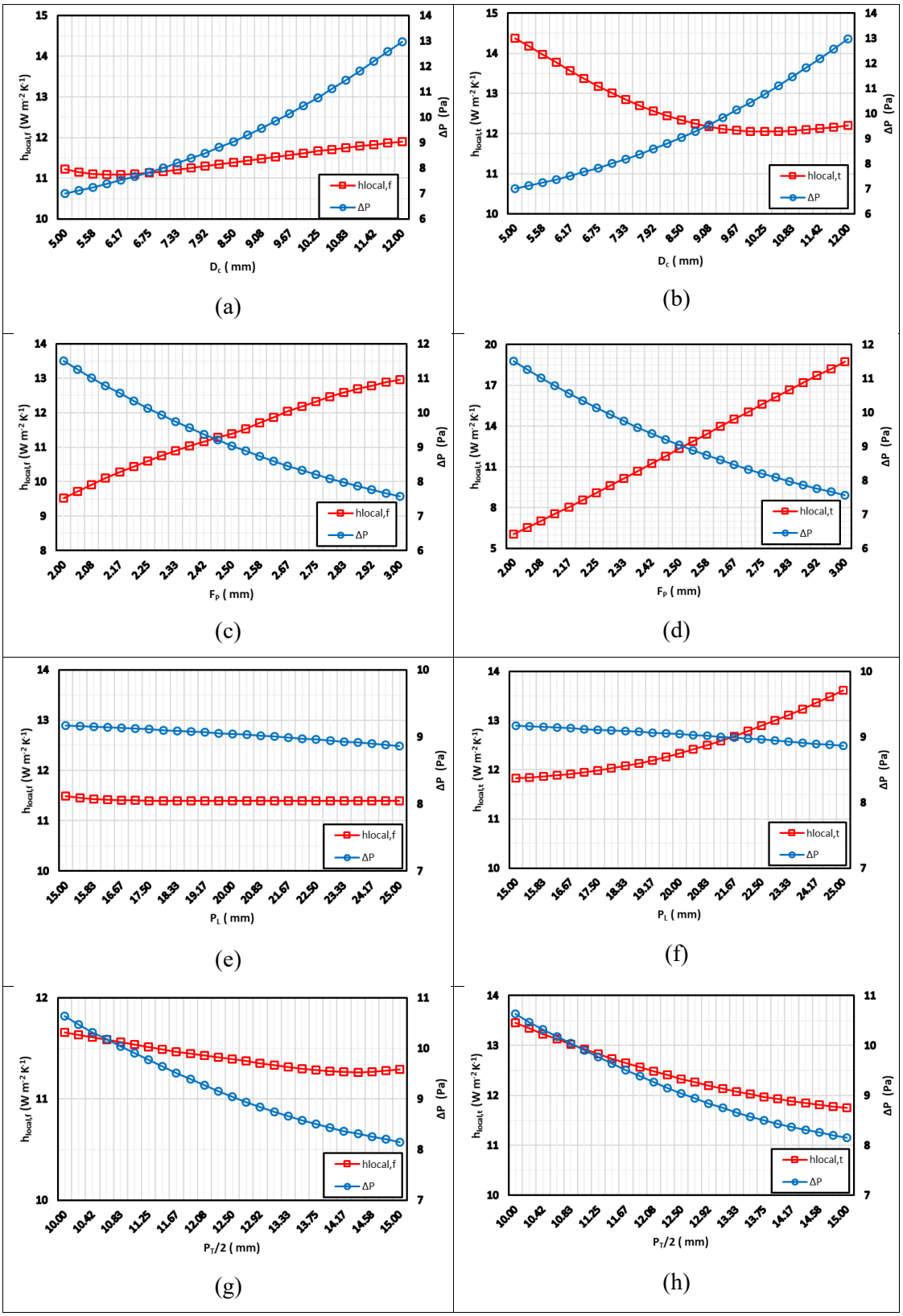


**Figure 6.** Effect of design parameters on the surface fin $h_{local,f}$ surface tube $h_{local,t}$ and ΔP at u = 1 m $s^{-1}$, a,b) effect of tube diameter, c,d) effect of fin pitch, e,f) effect of longitudinal pitch and g,h) effect of half transverse pitch

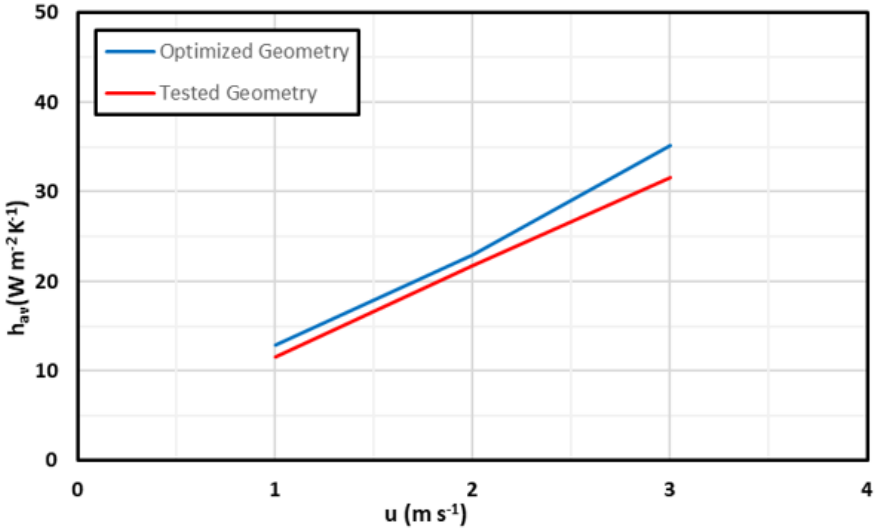


(a)

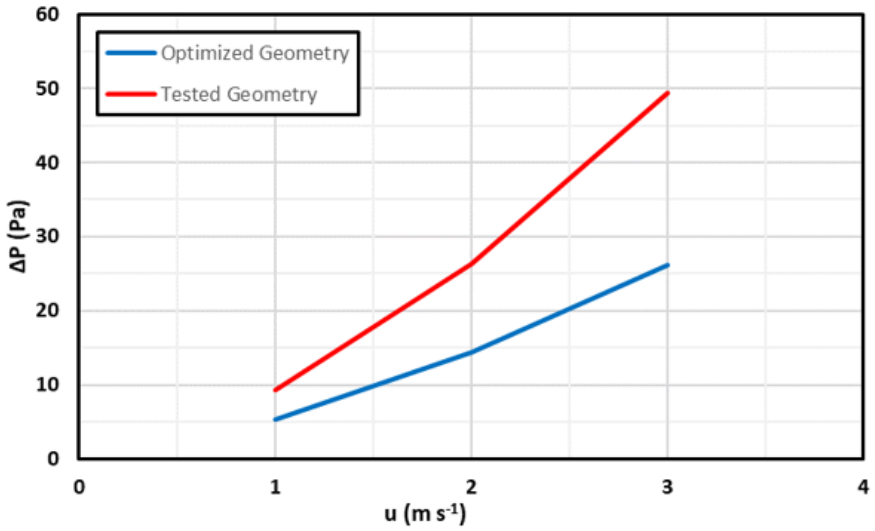


(b)

**Figure 7.** Thermal-hydraulic performance comparison between the optimum geometry and tested geometry; a) HTC, b) Pressure drop

The thermal-hydraulic performance comparison of the tested gas cooler and optimum gas cooler is shown in Figure 7 (a-b) below with regard to the HTC and pressure drop for three different inlet velocities. As can be noticed from Figure 7 (a-b), the optimum geometry has better thermal-hydraulic performance than the tested geometry. The overall HTC improvement is between 5.4 – 12.2 % whereas the pressure drop decreases about 175.08 – 188.58 % for three different inlet velocities. Considering the test condition inlet velocity of 2.55 m s$^{-1}$, the optimum geometry has almost 9.3 % greater HTC and 185 % fewer pressure drop in comparison with tested geometry.

## IV. CONCLUSIONS

In this study, the geometric optimization of the wavy fin gas cooler in $CO_2$ transcritical refrigeration system was performed using a multi-objective genetic algorithm. The three dimensional numerical model was validated with experiments. The numerical model fairly agreed (MAE 9.97 %) with

the experimental results in terms of total cooling capacity. Accordingly, four geometrical parameters longitudinal pitch, tube outer diameter, half of transverse pitch and fin pitch were optimized to have maximum cooling capacity and minimum pressure drop. The impact of each geometrical parameters on the surface HTC on the tubes and fins and pressure drop through the gas cooler was examined in details. The results evinced that the pressure loss and surface HTC on the fins and tubes are strictly related with these geometrical parameters. In this way, the geometry of the optimum gas cooler has obtained. It was found that the optimum gas cooler geometry exhibited greater HTC and lower pressure drop compared to tested geometry.

In this particular study four geometrical parameters are taken into account for optimization process since introducing more parameters to the simulation requires more powerful computers and causes excess computation time. For further investigations it is recommended that parameters such as wave inclination angle, wave amplitude and tube wall thickness should be taken into consideration in the optimization process.

## ACKNOWLEDGMENT

The authors would like to thank FRITERM Thermal Devices Inc. for their technical support.

## REFERENCES

**[1]** Bolaji, B. O., & Huan, Z. (2013). Ozone depletion and global warming: Case for the use of natural refrigerant–a review. *Renewable and Sustainable Energy Reviews*, 18, 49-54.

**[2]** Rony, R. U., Yang, H., Krishnan, S., & Song, J. (2019). Recent advances in transcritical CO2 (R744) heat pump system: a review. *Energies*, 12(3), 457.

**[3]** ASHRAE. 15 & 34 Safety Standard for Refrigeration Systems and Designation and Classification of Refrigerants ISO 5149 Mechanical Refrigerating Systems Used for Cooling and Heating—Safety Requirements.

**[4]** Lachner Jr, B. F., Nellis, G. F., & Reindl, D. T. (2007). The commercial feasibility of the use of water vapor as a refrigerant. *International Journal of Refrigeration*, 30(4), 699-708.

**[5]** American Society of Heating, Refrigerating and Air-Conditioning Engineers (2014). ASHRAE Position Document on Natural Refrigerants. Inc., Atlanta, GA, USA.

**[6]** Gullo, P., Hafner, A., & Banasiak, K. (2018). Transcritical R744 refrigeration systems for supermarket applications: Current status and future perspectives. *International Journal of Refrigeration*, 93, 269-310.

**[7]** Cecchinato, L., & Corradi, M. (2011). Transcritical carbon dioxide small commercial cooling applications analysis. *International Journal of Refrigeration*, 34(1), 50-62.

**[8]** Kılıç, B. (2018). Thermo-Economic Analysis of Transcritical Carbon Dioxide Refrigeration Cycle. *Avrupa Bilim ve Teknoloji Dergisi*, (14), 152-156.

**[9]** Jang, J. Y., & Chen, L. K. (1997). Numerical analysis of heat transfer and fluid flow in a three-dimensional wavy-fin and tube heat exchanger. *International Journal of Heat and Mass Transfer*, 40(16), 3981-3990.

**[10]** Kim, M. H., & Bullard, C. W. (2002). Air-side thermal hydraulic performance of multi-louvered fin aluminum heat exchangers. *International Journal of Refrigeration*, 25(3), 390-400.

**[11]** Mon, M. S., & Gross, U. (2004). Numerical study of fin-spacing effects in annular-finned tube heat exchangers. *International Journal of Heat and Mass Transfer*, 47(8-9), 1953-1964.

**[12]** Tao, Y. B., He, Y. L., Huang, J., Wu, Z. G., & Tao, W. Q. (2007). Numerical study of local heat transfer coefficient and fin efficiency of wavy fin-and-tube heat exchangers. *International Journal of Thermal Sciences*, 46(8), 768-778.

**[13]** Lu, C. W., Huang, J. M., Nien, W. C., & Wang, C. C. (2011). A numerical investigation of the geometric effects on the performance of plate finned-tube heat exchanger. *Energy Conversion and Management*, 52(3), 1638-1643.

**[14]** Dong, J., Su, L., Chen, Q., & Xu, W. (2013). Experimental study on thermal–hydraulic performance of a wavy fin-and-flat tube aluminum heat exchanger. *Applied Thermal Engineering*, 51(1-2), 32-39.

**[15]** Santosa, I. M., Gowreesunker, B. L., Tassou, S. A., Tsamos, K. M., & Ge, Y. (2017). Investigations into air and refrigerant side heat transfer coefficients of finned-tube CO2 gas coolers. *International Journal of Heat and Mass Transfer*, 107, 168-180.

**[16]** Zhang, X., Ge, Y., Sun, J., Li, L., & Tassou, S. A. (2019). CFD Modelling of Finned-tube CO2 Gas Cooler for Refrigeration Systems. *Energy Procedia*, 161, 275-282.

**[17]** Javaherdeh, K., Vaisi, A., & Moosavi, R. (2018). The effects of fin height, fin-tube contact thickness and louver length on the performance of a compact fin-and-tube heat exchanger. *International Journal of Heat and Technology*, 36(3), 825-834.

**[18]** Zhang, X., Ge, Y., & Sun, J. (2020). CFD performance analysis of finned-tube CO2 gas coolers with various inlet air flow patterns. *Energy and Built Environment*, 1(3), 233-241.

**[19]** European Committee for Standardization, (2014), Heat exchangers - Forced convection air cooled refrigerant condensers - Test procedures for establishing performance (CSN EN 327), Retrieved from https://www.en-standard.eu/csn-en-327-heat-exchangers-forced-convection-air-cooled-refrigerant-condensers-test-procedures-for-establishing-performance/

**[20]** European Committee for Standardization, (2014) Heat exchangers - Forced convection unit air coolers for refrigeration - Test procedures for establishing the performance (CSN EN 328), Retrieved from https://www.en-standard.eu/csn-en-328-heat-exchangers-forced-convection-unit-air-coolers-for-refrigeration-test-procedures-for-establishing-the-performance/

**[21]** Coleman, H. W., & Steele, W. G. (2018). Experimentation, Validation, and Uncertainty Analysis for Engineers. John Wiley & Sons, Haboken, NJ, USA.

**[22]** Fluent, A. (2009). Ansys Fluent 12.0 Theory Guide. ANSYS Inc., Canonsburg, PA.

**[23]** Menéndez-Pérez, A., Pita-Cantos, M. T. L., & Borrajo-Pérez, R. (2019). Determination of the optimum louver angle of a louvered fin with elliptical tubes. *Ingeniería Mecánica*, 22(1), 07-13.

**[24]** Gupta, A., Roy, A., Gupta, S., & Gupta, M. (2020). Numerical investigation towards implementation of punched winglet as vortex generator for performance improvement of a fin-and-tube heat exchanger. *International Journal of Heat and Mass Transfer*, 149, 119171.

**[25]** Bilir, L., Ozerdem, B., Erek, A., & Ilken, Z. (2010). Heat transfer and pressure drop characteristics of fin-tube heat exchangers with different types of vortex generator configurations. *Journal of Enhanced heat transfer*, 17(3).

**[26]** Okbaz, A., Pınarbaşı, A., Olcay, A. B., & Aksoy, M. H. (2018). An experimental, computational and flow visualization study on the air-side thermal and hydraulic performance of louvered fin and round tube heat exchangers. *International Journal of heat and Mass Transfer*, 121, 153-169.

**[27]** Balkanlı, B., Yurddaş, A., & Aksoy, Y. (2020). Split klimalarda kullanılan ısı değiştiricilerinde kanatçık etkisinin sayısal analizi. *Pamukkale Üniversitesi Mühendislik Bilimleri Dergisi*, 26(4), 689-699.

**[28]** Yeşil, Ç. (2007). Kanatlı borulardaki dış akış ve konjuge ısı transferi mekanizmasinin sayısal olarak incelenmesi. Yüksek Lisans Tezi, Yıldız Teknik Üniversitesi, Türkiye.

**[29]** Damavandi, M. D., Forouzanmehr, M., & Safikhani, H. (2017). Modeling and Pareto based multi-objective optimization of wavy fin-and-elliptical tube heat exchangers using CFD and NSGA-II algorithm. *Applied Thermal Engineering*, 111, 325-339.

**[30]** Box, G. E., & Draper, N. R. (1987). Empirical model-building and response surfaces. John Wiley & Sons.

**[31]** Kumari, M., & Gupta, S. K. (2019). Response surface methodological (RSM) approach for optimizing the removal of trihalomethanes (THMs) and its precursor's by surfactant modified magnetic nanoadsorbents (sMNP)-An endeavor to diminish probable cancer risk. *Scientific Reports*, 9(1), 1-11.

**[32]** Tang, S. Z., Wang, F. L., He, Y. L., Yu, Y., & Tong, Z. X. (2019). Parametric optimization of H-type finned tube with longitudinal vortex generators by response surface model and genetic algorithm. *Applied Energy*, 239, 908-918.

**[33]** Chavan, V., & Arakerimath, R. R. (2016). CFD Based Heat Transfer analysis of various Wavy Fin-and-Tube Heat Exchanger. *International Journal of Current Engineering and Technology*, (5), 258-261.

**[34]** Yin, J. M., Bullard, C. W., & Hrnjak, P. S. (2001). R-744 gas cooler model development and validation. *International Journal of Refrigeration*, 24(7), 692-701.

**[35]** Erek, A., Özerdem, B., Bilir, L., & Ilken, Z. (2005). Effect of geometrical parameters on heat transfer and pressure drop characteristics of plate fin and tube heat exchangers. *Applied Thermal Engineering*, 25(14-15), 2421-2431.

**[36]** Bhuiyan, A. A., Amin, M. R., Naser, J., & Islam, A. K. M. (2015). Effects of geometric parameters for wavy finned-tube heat exchanger in turbulent flow: a CFD modeling. *Frontiers in Heat and Mass Transfer (FHMT)*, 6(1).

**[37]** Romero-Méndez, R., Sen, M., Yang, K. T., & McClain, R. (2000). Effect of fin spacing on convection in a plate fin and tube heat exchanger. *International Journal of Heat and Mass Transfer*, 43(1), 39-51.

**[38]** Torikoshi, K., & Xi, G. N. (1995). A Numerical Steady of Flow and Thermal Fields in Finned Tube Heat Exchangers (Effect of the Tube Diameter). IMECE Proceedings of the ASME Heat Transfer Division, 317(1), 453-457.

**[39]** Tutar, M., & Akkoca, A. (2004). Numerical analysis of fluid flow and heat transfer characteristics in three-dimensional plate fin-and-tube heat exchangers. *Numerical Heat Transfer, Part A: Applications*, 46(3), 301-321.

**[40]** Watel, B., Harmand, S., & Desmet, B. (1999). Influence of flow velocity and fin spacing on the forced convective heat transfer from an annular-finned tube. *JSME International Journal Series B Fluids and Thermal Engineering*, 42(1), 56-64.

**[41]** Sparrow, E. M., & Samie, F. (1985). Heat transfer and pressure drop results for one-and two-row arrays of finned tubes. *International Journal of Heat and Mass Transfer*, 28(12), 2247-2259.

**[42]** Nir, A. (1991). Heat transfer and friction factor correlations for crossflow over staggered finned tube banks. *Heat Transfer Engineering*, 12(1), 43-58.